Journal of Volcanology and Geothermal Research 404 (2020) 107008

Contents lists available at ScienceDirect

Journal of Volcanology and Geothermal Research

journal homepage: www.elsevier.com/locate/jvolgeores

Fourier Shape Analysis, FSA: Freeware for quantitative study of particle morphology

G. Moreno Chávez [a], F. Castillo-Rivera [b], J.A. Montenegro-Ríos [c], L. Borselli [c,e], L.A. Rodríguez-Sedano [b], D. Sarocchi [c,d,*]

[a] Maestría en Ciencias del Procesamiento de la Información, Universidad Autónoma de Zacatecas, Av. Ramón López Velarte 801, Zacatecas 98000, Mexico
[b] CONACYT-Instituto de Geología, Universidad Autónoma de San Luis Potosí, Av. Dr. M. Nava No 5, Zona Universitaria, 78290 San Luis Potosí, Mexico
[c] Instituto de Geología/Facultad de Ingeniería, UASLP, Av. Dr. M. Nava No 5, Zona Universitaria, 78290 San Luis Potosí, Mexico
[d] Department of Geosciences, Boise State University, 1910 University Drive, Boise, ID 83725-1535, United States
[e] Dipartimento di Scienze della Terra (DST), Universitá degli Studi di Firenze, Via la Pira 4, 50121 Firenze, Italy

ARTICLE INFO

Article history:
Received 4 March 2020
Received in revised form 20 July 2020
Accepted 24 July 2020
Available online 1 August 2020

Keywords:
Fourier shape analysis
Particle morphology
Fourier shape parameter optimization
Fourier Shape Analysis software
Pyroclastic deposit characterization

ABSTRACT

Shape analysis is of paramount importance in sedimentology. Particle morphology is a very useful texture parameter that provides information about particle history and is used to characterize and classify sedimentary material. Particle shape description has been both an important and a controversial subject. The most convincing description of shape defines particle shape by three hierarchical parameters: form, roundness, and surface texture (Barrett, 1980). Many different methods have been proposed to measure these parameters. Among them, Fourier shape analysis is particularly notable. Fourier analysis separates the three parameters into frequency ranges. The low frequency range is related to form, the middle frequency range to roundness and the high frequency to surface texture. However, determining where the boundaries lie between the different morphological classes is not an easy task and has been an unsolvable problem since the FSA method was first proposed. The same is true for the signal-to-noise limit. To date, this information has been obtained empirically and with great uncertainty. One of the most important contributions of this work has been to quantitatively constrain the harmonic ranges corresponding to the morphological ranges proposed by Barrett, and to determine the best possible approximation for the upper limit of the signal and the onset of noise. To estimate these ranges, we propose here two original methodologies based on analysis of the cumulative amplitude spectrum (CAS), and on simulating the effect of artificial noise acting on a well-known geometric figure. The CAS of 3664 volcaniclastic particles and of 106 artificially silhouette charts have been quadrisected into form, roundness, roughness and noise using an optimization process. The analysis indicates overall that the limits are well constrained into a narrow range of harmonics with a small variance. The results obtained are reliable and allow the range of harmonics that contains a useful signal to be extended up to harmonic 256. The method has been successfully applied to the standard figures of Krumbein (1941a) and of Powers (1953), efficiently separating the different classes of roundness. As an example, the methodology has been applied to a real-life case where there was doubt about the pristine nature of the materials from some outcrops related to the block-and-ash flow deposit of the July 17, 1999 eruption of the Colima volcano. The results obtained applying the method show promising results, indicating the potential of FSA information to solve this ambiguity. The powerful, user-friendly FSA software that we distribute freely (open code) can be very useful for characterizing volcano-sedimentary and sedimentary deposits. To date, there is no other software for FSA studies. Moreover, FSA can be useful in other fields of science and engineering where quantitative particle shape analysis is needed.

1. Introduction

Particle morphology (PM) is of great interest in earth science and several other scientific fields and engineering disciplines. PM in sedimentology is a very useful shape parameter that contains information about the processes that the particle has undergone since its formation and during transport and deposition (Krumbein, 1941a; Lukas, 2013). This textural characteristic is the consequence of various processes involving a set of particles, such as collisions, abrasion, friction, comminution, exposure time, and pathway, among others (Krumbein, 1941b; Caballero et al., 2012; Caballero et al., 2014).

* Corresponding author at: Instituto de Geología/Facultad de Ingeniería, UASLP, Av. Dr. M. Nava No 5, Zona Universitaria, 78290 San Luis Potosí, Mexico.
E-mail address: damiano.sarocchi@uaslp.mx (D. Sarocchi).

https://doi.org/10.1016/j.jvolgeores.2020.107008
0377-0273/

PM provides very useful data for volcanologists. The field of application spans several areas of explosive volcanism; for example, the study of ash particles in the atmosphere, in which the aerodynamic behavior of the particles also depends on particle shape (Dellino et al., 2012; Cioni et al., 2014; Leibrandt and LePennec, 2015), or the study of pyroclastic deposits, where particle morphology provides key information about the magmatic or hydromagmatic nature of an eruption (Wohletz, 1983; Heiken and Wohletz, 1985). Particle shape also provides important information about the processes that occur in pyroclastic density currents (PDC) or debris flows (DF). Particle shape enables inferences about the flow rheology, the type of inter-particle contact (i.e., collisional or frictional regime), and the kinetic and mechanical energy involved in such interactions (Maria and Carey, 2007; Manga et al., 2011; Sarocchi et al., 2011). The type of interaction between particles changes in the presence of water within the granular flow, determining whether the morphologies are more rounded and smoothed, or less so. This can, for example, help to discriminate between reworked and primary deposits, a problem that the sediment volcanologist often faces. Finally, particle morphology enables a better understanding of the physical phenomena associated with the volcanic process and the characterization and correlation of pyroclastic and epiclastic deposits.

The concept of particle shape is complex. Shape can have different meanings in relation to the external morphology of a body (Winkelmolen, 1982). After decades of discussions starting at the beginning of the twentieth century with the pioneering studies of Wentworth (1919), Wadell (1933) and Krumbein (1941a), a hierarchical concept of particle morphology was developed by Barrett (1980). According to Barrett, particle morphology is expressed by three independent properties acting on different scales (orders of magnitude); form (overall shape), roundness (large-scale smoothness) and surface texture (or roughness). Form is a first-order property; it records variations at the full particle scale. Roundness is a second-order property superimposed on overall form. It reflects variations related to the sharpness of the edges and the number of corners (Barrett, 1980; Lees, 1964; Powers, 1953; Krumbein, 1941a, 1941b). Surface texture is a third-order property, superimposed on the perimeter edges and the overall form. It relates to smaller scale features; for example, asperities of the surface and finer irregularities, and is used to describe the surface roughness, degree of polish, greasiness, and scratches (Alshibli and Alsaleh, 2004; Barrett, 1980). These properties are related in a hierarchical order and do not affect each other. The type of material constituting the particles, transport abrasion, interparticle friction, and chemical alteration contribute mainly to the latter two properties. These characteristics are illustrated in hierarchical order in Fig. 1.

The study of particle shape in volcanology dates back to the pioneering studies of Wohletz (1983) and Heiken and Wohletz (1985), who established a relationship between clast morphology and the characteristics of explosive eruptions. These studies, fundamental for the characterization of hydro-magmatic deposits, were only qualitative or semi-quantitative. However, a quantitative automated study of particle morphology is very important, as it enables a larger set of particles to be treated using a statistical approach, providing more precise and reliable results as well as parameters more sensitive to small shape variations.

In the 1990s, the spread of personal computers and the emergence of image analysis programs generated a new interest in particle morphology analysis (Russ, 1990; Kaye, 1999). In volcanology, as in many other disciplines, progressively more studies using these novel technologies emerged (Bayhurst et al., 1994; Capaccioni and Sarocchi, 1996; Dellino and La Volpe, 1996). The studies were carried out on 2D sections of the clasts, with the particles in resting position or with random cuts

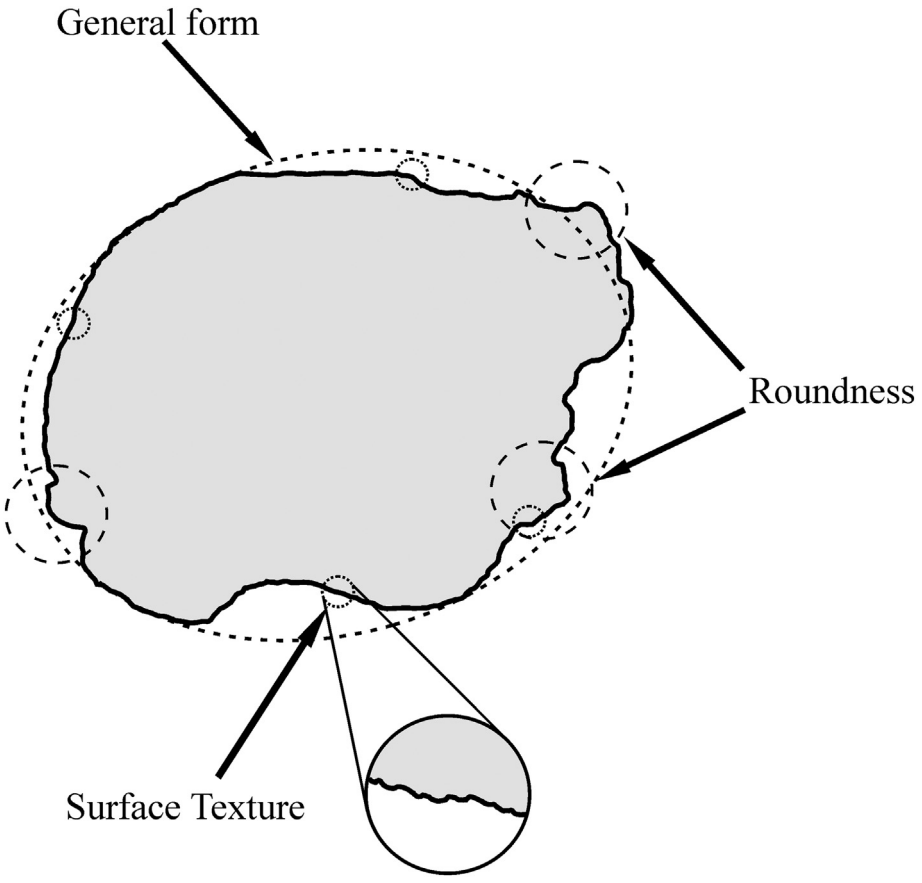

Fig. 1. The figure shows the particle outline with the features corresponding to irregularities of different orders (form, roundness, and texture). These properties are superimposed in hierarchical order and do not affect each other.

along polished slabs. This methodology continues to this day in most of the studies carried out, by virtue of its proven accuracy and simplicity (Tunwal et al., 2020).

A wide set of morphological coefficients have been used in volcanology through the years. Initially, given the limitations of computers for image analysis in the 1990s, the morphological parameters used were based mainly on simple geometric characteristics extracted from 2D features, such as area, perimeter and axis lengths. Combined, these metrics provided dimensionless parameters able to describe different shapes. Among these, the parameters of convexity, circularity, solidity, compactness, elongation and aspect ratio were particularly useful (Capaccioni and Sarocchi, 1996; Dellino and La Volpe, 1996; Leibrandt and LePennec, 2015; Tunwal et al., 2020). With the passing of time and the increase in computing power, other more complex and efficient parameters have been proposed. These include box counting fractal dimension and compass fractal dimension (Maria and Carey, 2002; Scasso and Carey, 2005; Tunwal et al., 2020), multifractal object characteristics (Dellino and Liotino, 2002; Sarocchi et al., 2011), and Fourier shape analysis (FSA) (Sarocchi et al., 2011; Charpentier et al., 2013). The following sections will examine the latter in more detail.

Recently the possibility of obtaining 3D particle morphology parameters by means of different methodologies has been explored, although this is a field where more development is needed. Pseudo-3D analysis of particle morphology based on matter–light interactions (Ersoy, 2010) has been explored. Other authors used shape from shadow methodology (Montenegro Ríos et al., 2013), providing dimensionless 3D parameters. New methods such as X-ray microcomputed tomography can provide very complete 3D morphological studies (Erdoğan et al., 2007; Bagheri et al., 2015) and this promises to be the future standard of morphometric analysis for volcanic particles. However, to date, X-ray microtomography instruments are still too expensive for most laboratories around the world. For this reason, 2D particle morphology methods based on fractal or Fourier analysis will be useful in volcanology for some years more.

The method of analyzing particle perimeters using Fourier transform analysis is based on the universally used mathematical tool developed by Jean Baptiste Fourier in the nineteenth century (Bracewell, 1986). Fourier demonstrated that any time series, even if it has infinite period and is bijective, can be represented by a series of sinusoidal functions (Davis, 1986). The Fourier transform enables a periodic function to be decomposed into the sinusoidal functions of different frequency, amplitude and phase that constitute it. Schwarcz and Shane (1969) and Ehrlich and Weinberg (1970) were pioneers in applying the Fourier method to geology, analyzing the perimeters of particle sections by means of time series, and successfully relating the harmonic amplitude to different kinds of morphological irregularity (see Section 3). Starting in the 1980s, the spread of personal computers with sufficient computing power for running Fourier shape analysis (FSA) programs made the application of this method to different fields of sedimentology possible (Full et al., 1984; Mazzullo et al., 1986; Haines and Mazzullo, 1988; Diepenbroek et al., 1992; Barclay and Buckingham, 2009; Sarocchi et al., 2011; Caballero et al., 2012; Charpentier et al., 2013).

The FSA method provides a spectrum where the harmonics are related to different types of irregularities (Sarocchi et al., 2011). The lowest order harmonics are related to the general form of the particle's perimeter and the highest order harmonics to finer aspects of the surface (e.g., texture). However, a challenge with this method has always been finding the relationship between the information provided by the harmonics and the shape orders considered to date (Ehrlich and Weinberg, 1970; Full et al., 1984); for example, the hierarchical ranges proposed by Barrett (1980).

Despite the potential of the FSA method for quantitative study of pyroclastic and epiclastic clast morphology, there are no commercial programs, and even less freeware, that enable this type of study to be carried out. Researchers who have worked with this methodology to date (Full et al., 1984; Mazzullo et al., 1986; Haines and Mazzullo, 1988, Diepenbroek et al., 1992; Barclay and Buckingham, 2009; Sarocchi et al., 2011; Caballero et al., 2012; Charpentier et al., 2013; Caballero et al., 2014) have developed their own software, and in most cases these programs are not available to the community.

Among the most important objectives of our study is solving the long-standing problem of which harmonics provide information for specific ranges of shape (e.g., form, roundness, roughness) and up to which harmonica useful signal is available. The other important contribution of this work is to provide the scientific community with friendly, powerful, versatile and freely distributed software to undertake FSA clast morphology analysis. Both problems have been solved and are explained in the following sections.

2. Material and methods

The code used for the optimization procedure has been developed in Matlab 2014b and can be downloaded and edited in the repository https://github.com/Gamalielmch/FSA. The executable software (FSA), available for PC under the Windows operating system, is described in Appendix A, and can be downloaded from our website http://www.laima-uaslp.org/descargas.html.

2.1. Fourier framework

The FSA technique basically consists in converting the particle's perimeter (2D) into a signal (1D) by using the intersection between a straight line segment l_n through the origin in the centroid (c) of the particle and a section of its contour (x_n, y_n) (see Fig. 2). This procedure (presented in following paragraphs) is known as the (R,θ) method. The sampling along the perimeter must be equally spaced (usually by interpolation) and each segment l_n is associated with exactly one element of the contour (x_n, y_n). The signal is processed by a fast Fourier transform and then the amplitude spectrum is analyzed to characterize the morphology of the particle (Schwarcz and Shane, 1969; Ehrlich and Weinberg, 1970; Sarocchi et al., 2011; Charpentier et al., 2013). A general description of the mathematical procedure is as follows.

The perimeter of the particle is obtained from a digital image. The perimeter corresponds to the pixels of the particle's contour, which are obtained by segmentation. The image is segmented using Otsu's method (Otsu, 1979). Let $P = \{p_0, p_1, \ldots, p_{N-1}\}$ be the set of pixels of the perimeter and let l_n be the length of the segment between the centroid c and p_n. Here N is the total number of pixels of the perimeter and $n = 0, 1, 2, 3, \ldots, N - 1$. The x-centroid is estimated by $c_x = \frac{1}{6A}\sum_{n=0}^{N-1}(x_n + x_{n+1})(x_n y_{n+1} - x_{n+1} y_n)$ and y-centroid by $c_y = \frac{1}{6A}\sum_{n=0}^{N-1}(y_n + y_{n+1})(x_n y_{n+1} - x_{n+1} y_n)$ where A is the area of the particle and (x_n,y_n) is the Cartesian position of p_n. The function that takes all possible values of the perimeter (Fig. 2) is denoted by $r(\theta)$, where $\theta = (0, 2\pi]$ is the angle between the element p_n and the horizontal axis. To estimate the discrete Fourier transform (DFT) of $r(\theta)$, this function must be bijective $r(\theta_n) \in \{p_n\}$, and with equally spaced sampling points, $\Delta\theta = Constant$ along the perimeter. Generally, when a segment l_n intersects more than one element of P, the first, the last, or the mean intersection is selected. Here, we use the mean intersection, which is calculated by $p_n = \frac{1}{T}\sum_{t=1}^{T}|c - p_n^t|$, where $\{p_n^1, p_n^2, \ldots, p_n^t\}$ is the set of pixels that are intersected by a given angle θ. The equally spaced sampling $\Delta\theta = 2\pi/N$ is achieved using the nearest-neighbor interpolation (NNI) process.

The NNI method assigns the nearest x_n given θ_n; namely, $r(\theta_n) = \min\{|c - p_0|, |c - p_1|, \ldots, |c - p_{N-1}|\}$, where equally spaced sampling is given by $\theta_n = 2\pi n/N$. The Fourier transform is applied to the $r(\theta)$ function as follows:

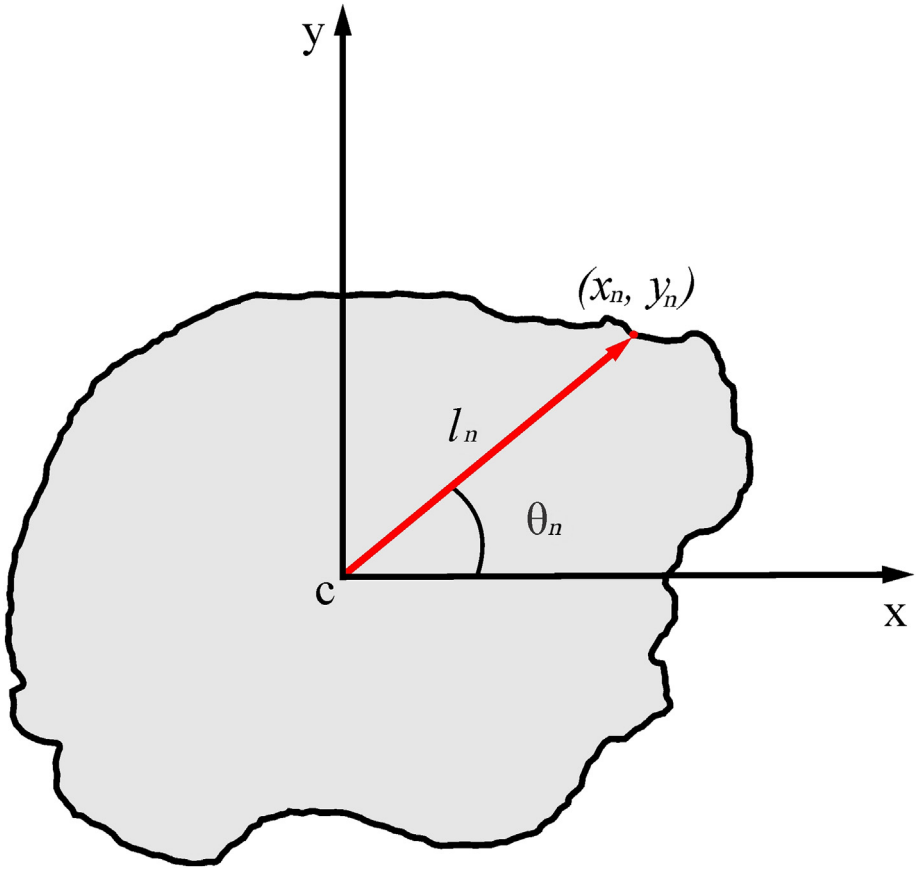

Fig. 2. Schematic representation of how the perimeter contour of a particle is acquired. Illustration adapted from Barrett (1980).

The NNI method assigns the nearest x_n given θ_n; namely $r(\theta_n) = \min\{|c - p_0|, |c - p_1|, \ldots, |c - p_{N-1}|\}$, where equally spaced sampling is given by $\theta_n = 2\pi n/N$. The Fourier transform is applied to the $r(\theta)$ function as follows:

$$R(k) = \sum_{n=0}^{N-1} r(\theta_n) e^{-j\omega_k n}, \quad (1)$$

where j is a complex variable, ω is the frequency, which is calculated for each harmonic k by $\omega_k = 2\pi k/N$, $k = 0, 1, \ldots, N-1$; thus $R(k)$ is the DFT of the perimeter of the particle.

It is well known that the Fourier transform can be expressed by its phase $\angle R(k)$ and magnitude $M(k) = |R(k)|$ response (Proakis and Manolakis, 2004) To characterize the shape of the particle, we use the magnitude response (amplitude spectrum). The magnitude of the different harmonics is related to different orders of shape (according to Barrett, 1980). Low order harmonics are related to general aspects of shape, and progressively higher order harmonics correspond to progressively finer irregularities, vanishing into noise. As described in several works (Schwarcz and Shane, 1969; Ehrlich and Weinberg, 1970; Caballero et al., 2012; Charpentier et al., 2013), the magnitude spectrum can be trisected in order to associate each section with a morphological characteristic; namely, the first section with form, the second with roundness and the third with surface texture (roughness). In addition to these divisions, we have included Section 3.2 corresponding to digital noise, as shown in Fig. 4. Section 3.2 was estimated to focus on the resolution of the particle image, which is related to the number of pixels constituting the perimeter.

3. Procedures to determine harmonic ranges associated with shape orders and noise

In this section, we introduce the procedures developed to determine the harmonic thresholds that separate different shape components and to identify where the signal vanishes, and noise begins.

3.1. Form, roundness, and roughness thresholds

The thresholds in the Fourier spectrum amplitude delimit ranges corresponding to different types of irregularities (Schwarcz and Shane, 1969). In the past, according to the literature, the thresholds have been chosen arbitrarily (Schwarcz and Shane, 1969; Ehrlich and Weinberg, 1970; Haines and Mazzullo, 1988; Sarocchi et al., 2011; Caballero et al., 2012). To improve on this method, we propose an unbiased quantitative approach to estimate the thresholds between shape components. The three shape parameters, according to Barret, are independent; this means that they do not affect each other. Therefore, the shape parameters are distinguished by a change in the order of magnitude. The change in order can be detected by changes in the slope of the cumulative amplitude spectrum (CAS) curve (Fig. 3A, for example). The CAS is calculated using the expression $C(K) = \sum_{k=0}^{K} M(k)$. If the increase in the curve is constant, the harmonics are of the same order. On the other hand, if the slope decreases enough, an inflection point is generated. This point represents a change in the order of magnitude. After the inflection point, the slope is notably less. Fig. 3 shows an example of the CAS curve. The red and blue lines are mapping each harmonic in the CAS to detect inflection points (see next paragraph).

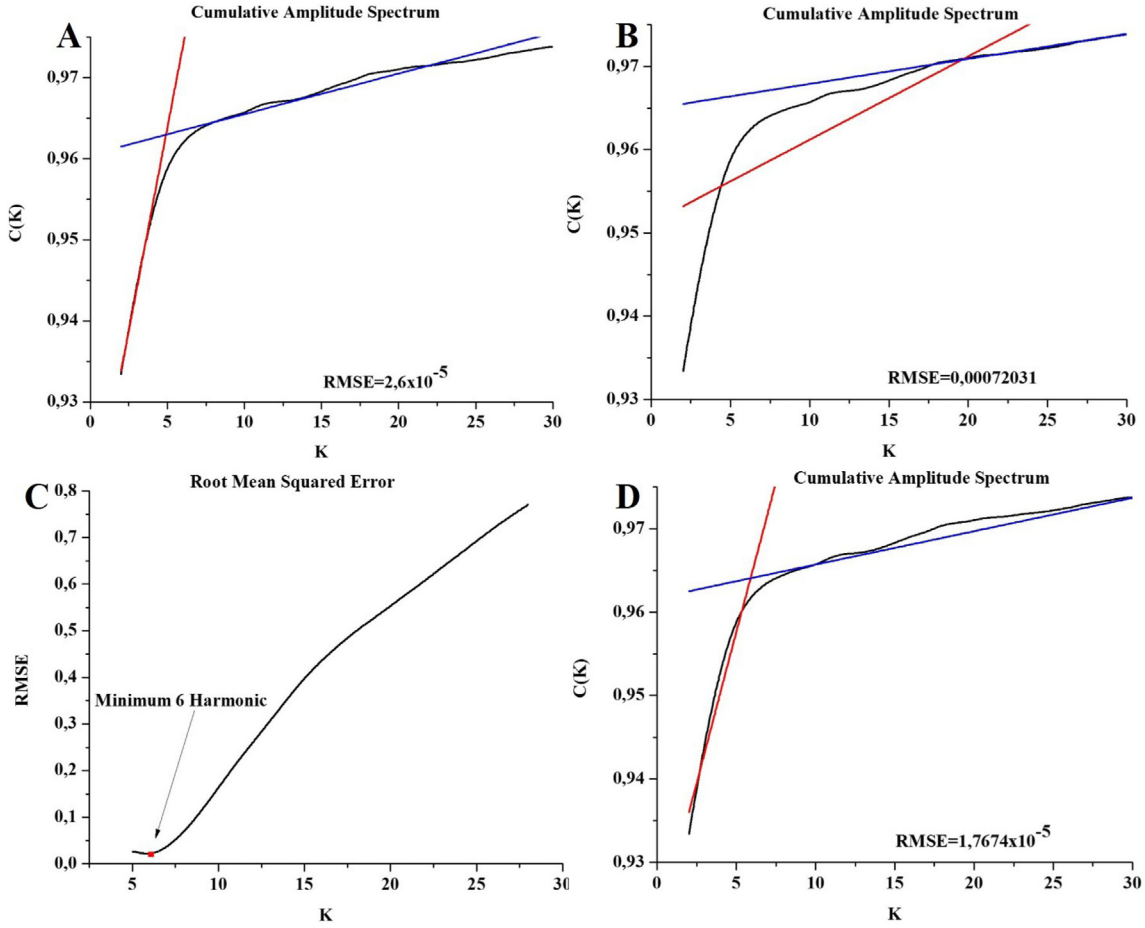

Fig. 3. Example of a typical cumulative amplitude spectrum curve and its bisection using L-method. The bisection by harmonics 5 and 20 is shown in (A) and (B) respectively. Fig. A and B shown a good and poor example of curve fitting. The RMSE for all harmonics is shown in (C) where the minimum corresponds to harmonic 6. Finally, in (D) The two-straight line for RMSE minimum are shown.

To determine the harmonic at which the order of magnitude changes, we propose an optimization function based on the L-method (Salvador and Chan, 2004) and the method proposed by Borselli (1999). The CAS is bisected by a harmonic. Each part is fitted by a straight line (Fig. 3A) and the root mean squared error (RMSE) is calculated. Fig. 3A and B shows examples of a good and poor fit respectively as well as their RMSE. This procedure is repeated for all harmonics. The harmonic with the lowest RMSE (Fig. 3C) will be the inflection point (threshold). Before this inflection point, we assign one type of irregularity (general form, roundness, or roughness) and after the point another one is assigned. An example of the best-fit procedure is shown in Fig. 3D.

The objective function proposed for this calculation is the following:

$$Q(\alpha_1,\beta_1,\alpha_2,\beta_2,a) = \sum_{k=ai}^{a} |C(k)-\alpha_1 k-\beta_1|^2 + \sum_{k=a+1}^{af} |C(k)-\alpha_2 k-\beta_2|^2, \quad (2)$$

where α_1 and β_1 are the slope and intersection of the ordinates of the linear fit of the left-hand side $C(a_i,\ldots,a)$ respectively, and α_2 and β_2 the linear fit of the right-hand side $C(a+1,\ldots,a_f)$ respectively, and "a" is the harmonic that bisected the curve. The value "a" that minimizes the function is the threshold. This procedure is applied to obtain the threshold between form and roundness.

The form is determined by the first harmonics. We have found that to estimate the form threshold it is enough to analyze the first 12 harmonics. Using more than 12 coefficients will only slow down the processing. The range to calculate the form threshold is then $a_i = 2$ and $a_f = 12$. The harmonic 1 is discarded because it is related to the size of the clast. The initial harmonic of the range to estimate the roundness threshold is the threshold of the form, a harmonic between 2 and 12. The final harmonic for the roundness range will be the roughness threshold. The roughness threshold is calculated using Eq. (3) (see Section 3.2).

The only constraint on the objective function is that the linear fitting must have at least 3 points. This constraint is based on the fact that the form must include at least 3 harmonics. The optimization problem is solved by an exhaustive search. In cases where there is more than one minimum, the lowest harmonic is chosen, because the form is defined by the lowest frequencies. An example of threshold estimation using this procedure is shown in Fig. 4.

3.2. Effects of image resolution on the textural surface parameter and noise

As we mentioned in the previous section, surface texture (roughness) is the third-order shape class and corresponds to the highest frequency range. However, digital noise related to the image quantization process is present in the same frequency range.

The maximum observable frequency (MOF), related to the highest harmonic containing useful information, is calculated according to Nyquist's theorem (Nyquist, 2002). The MOF in a signal is half the sampling frequency. For the proposed analysis, the sampling frequency is directly proportional to the number of pixels in the perimeter of the particle image. The resolution at which a particle has been digitized

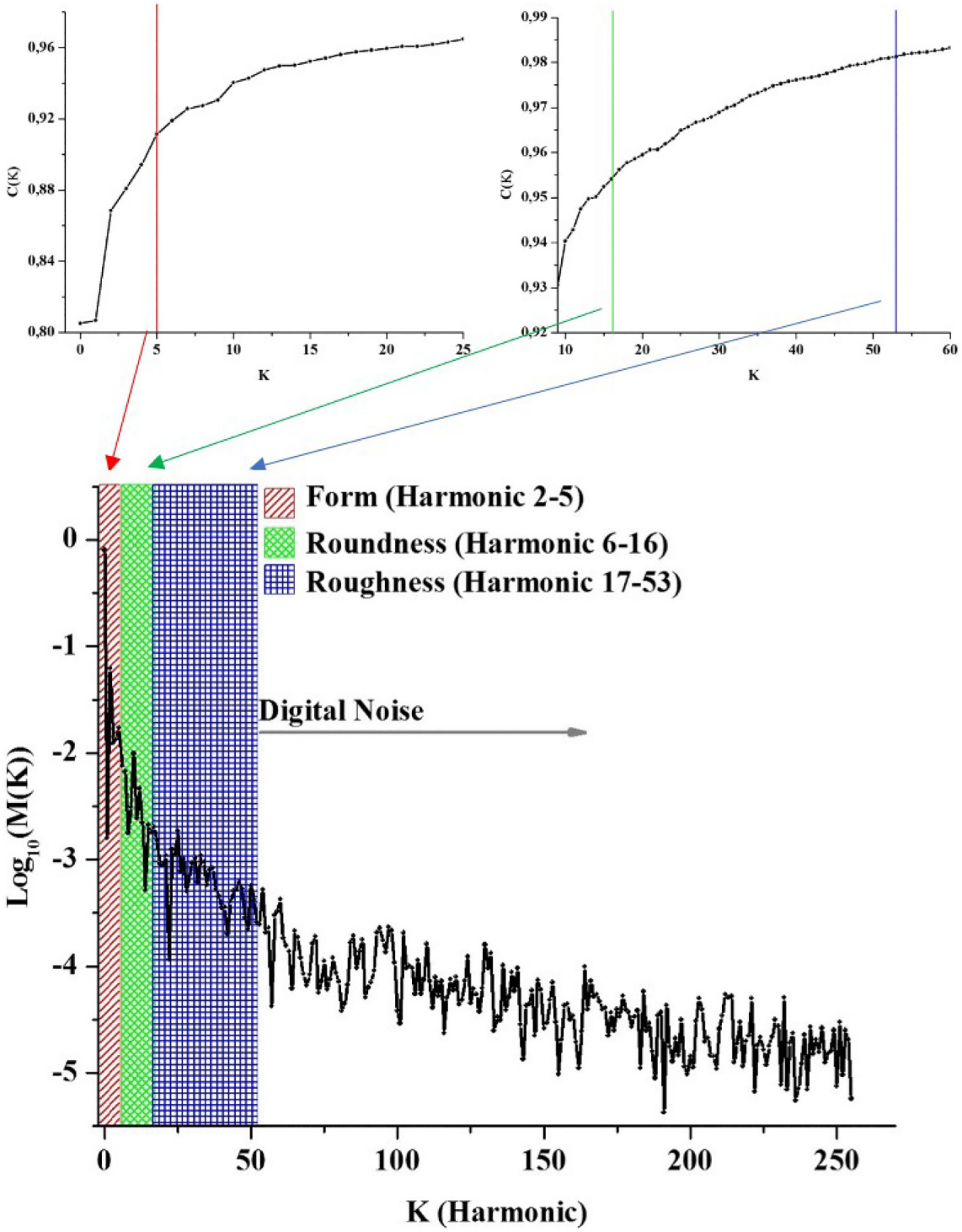

Fig. 4. Example of threshold estimation. The form (red area) and roundness (green area) thresholds are estimated by the proposed optimization method. The thresholds for surface texture (blue area) and digital noise (indicated by the gray arrow) are calculated by Eq. (3). The parameter M(k) is the magnitude of the harmonic k.

determines this number of pixels and therefore the MOF. Using this concept, we attempt to solve an important and controversial aspect of the threshold between surface texture and digital noise (Schwarcz and Shane, 1969; Diepenbroek et al., 1992; Barclay and Buckingham, 2009; Sarocchi et al., 2011).

In order to evaluate the effect of image resolution on noise and to understand at which frequencies noise overcomes the signal related to particle irregularities, a computer simulation was carried out. A sinusoidal signal simulating irregularity was superimposed on a simple shape, a circle. Several images were produced with different irregularities, simulating the three morphological orders: form, roundness and roughness. Fig. 5 shows the example of a circle with a perimeter composed of 628 pixels, on which progressively finer irregularities have been overlapped (Fig. 5A to F). Depending on the frequency of the superimposed sinusoidal signal, perimeter deformation determines the change of irregularity. Morphologies

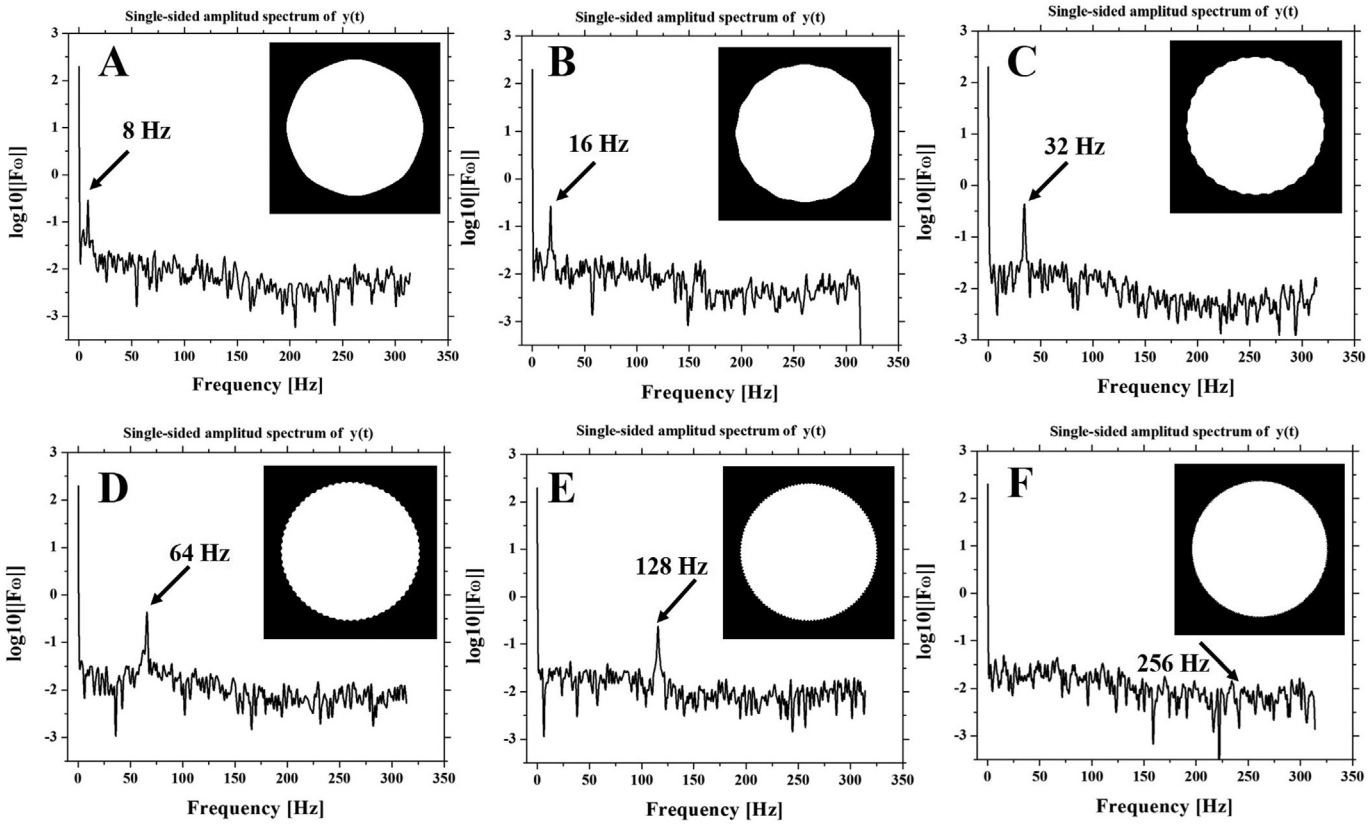

Fig. 5. Spectra corresponding to a circle with a 628-pixel perimeter, deformed by a superimposed sinusoidal signal. Based on the Nyquist sampling theorem, the maximum detectable frequency (MOF, indicated by arrows) is 314 Hz. In (A) the superimposed frequency is located at 8 Hz, in (B) at 16 Hz, (C) at 32 Hz, (D) at 64 Hz, (E) at 128 Hz and (F) at 256 Hz. Note how with higher order harmonics, the peak is less marked and disappears among the noise.

correspond to the order of "form" (Fig. 5A), "roundness" (Fig. 5B and C) and "roughness" (Fig. 5D to F).

The sinusoidal signal produces a well-defined peak in the Fourier spectra (see Fig. 6). As the frequency of the superimposed irregularities increases, the peak moves towards higher order harmonics. Observing Fig. 5 from A to F, it can be seen that the peak is progressively less pronounced and disappears when noise overcomes it. The harmonic at which the signal corresponds to the artificial irregularity is lower than the image discretization noise corresponding to the MOF. This value, indicating the last harmonic containing morphological information, varies depending on the image resolution.

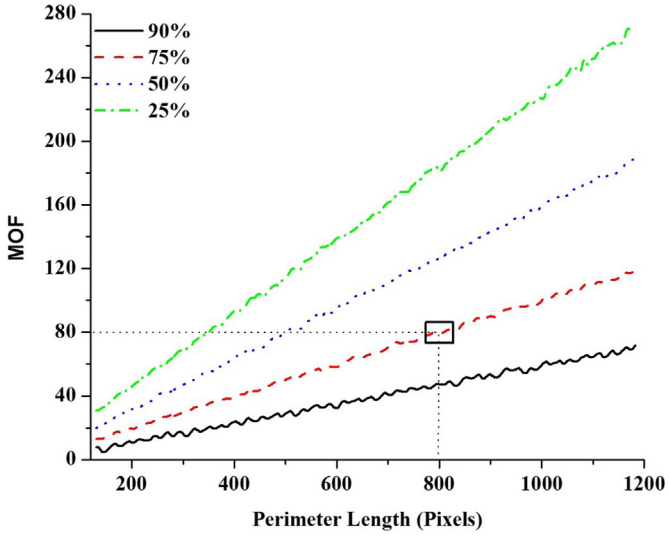

Fig. 6. Curves relating MOF harmonics of the disturbed series of circles to perimeter length (pixels) determined by image resolution. Different curves represent different percentages of signal magnitude preserved. The results show that increasing the image resolution increases the number of harmonics containing a useful signal. These curves can be used to determine the MOF harmonic (where noise starts) as a function of image resolution.

The results of the simulation are summarized in Fig. 6. The curves in Fig. 6 enable the maximum harmonic with useful morphological information to be determined as a function of the object perimeter length (related to resolution) and the amount of morphological information we want to preserve (90%, 75%, 50% or 25%). If the resolution of the image is increased, the useful information (MOF) moves towards harmonics of higher order. For example, if we want to preserve 75% of the magnitude of the spectrum for a resolution of 800 pixels, the graph in Fig. 6 indicates that we need approximately 80 harmonics (red line).

The curves shown in Fig. 6 are useful for determining the threshold between surface texture (roughness) signal and noise. The threshold suggested in this work is the harmonic at which 75% of the signal magnitude is preserved. This percentage is conservative and guarantees a clear distinction between noise and an irregularity corresponding to the shape. To incorporate this procedure into the proposed algorithm, a curve was fit to the 75% magnitude curve. The expression is given by

$$H(P) = 0.1005P - 0.4424, \quad (3)$$

where H(P) is the MOF harmonic given by the number of pixels (P) in the perimeter. Then the threshold between roughness and noise is given by ths = ⌈H(P)⌉.

The result of the optimization process and the statistical study was carried out using a sample of more than three thousand volcanic clasts

Table 1
Harmonic thresholds between form and roundness and between roundness and roughness, obtained by the optimization methods for three different sets of clasts, natural and artificially designed.

	Number of clasts	Form/roundness by optimization	Roundness/roughness by optimization	Roughness/noise numerical
Set of natural volcaniclastic particles	3664	5 ± 0.9	20 ± 6	82 ± 32.5
Set of Krumbein reference figures	81	5 ± 0.7	18 ± 4.7	73 ± 4.9
Set of Power, Taylor and Pettijohn reference figures	25	5 ± 0.9	15 ± 5.5	76 ± 7.2

distributed among the categories pumice pyroclastic fall (30%), block and ash flow (22%), debris avalanche (15%), lahars (15%), lithic pyroclastic fall (11%), and artificially fractured basaltic rocks (7%). This study shows that all the thresholds, despite certain variability, are concentrated in specific harmonic ranges (Table 1). In general, it can be noted that in more regular and rounded clasts, all thresholds (form, roundness and roughness) move slightly towards the lower harmonics, while with more irregular and angular particles, all thresholds shift towards higher values (see Fig. 7). The statistically more representative thresholds are located at harmonic 5 ± 0.9 dividing "form" from "roundness", and 20 ± 6 dividing "roundness" from "roughness."

As a cross-test, the same analysis by optimization was performed using the 81 artificial reference figures constructed by Krumbein (1941a, 1941b) and the 25 constructed by Powers (1953). The results (Table 1) show that the form/roundness and roundness/roughness thresholds fall in the same range of harmonics for all data sets.

In Fig. 7, some examples of very different natural clast shapes are presented with their corresponding morphological thresholds. The results are in agreement with the study carried out using the large set of natural particles.

4. Testing the method

In this section, the results obtained from applying the FSA algorithm to Krumbein's and Pettijohn's reference figures are shown, as well as an example of a practical application of FSA parameters to a real geological case study.

4.1. Roundness test with Krumbein's and Powers's comparative silhouettes

In order to demonstrate the usefulness of the proposed algorithm, a "roundness" classification test was carried out, applying FSA to the silhouettes of the artificial clasts (Appendix B Figs. B.1 and B.2) proposed by Krumbein (1941a, 1941b), Powers (1953), and Muller (1967). Visual silhouettes have been used for many years as a semi-quantitative method for the evaluation of clast roundness in sedimentary deposits and can be considered a reference standard for roundness (Lewis and McConchie, 1994; Tucker, 2009).

The graphs in Fig. 8A–B show the results of the FSA analysis using the harmonic range 6–20 corresponding to roundness. The morphological coefficient MC6–20 can discriminate efficiently between images based

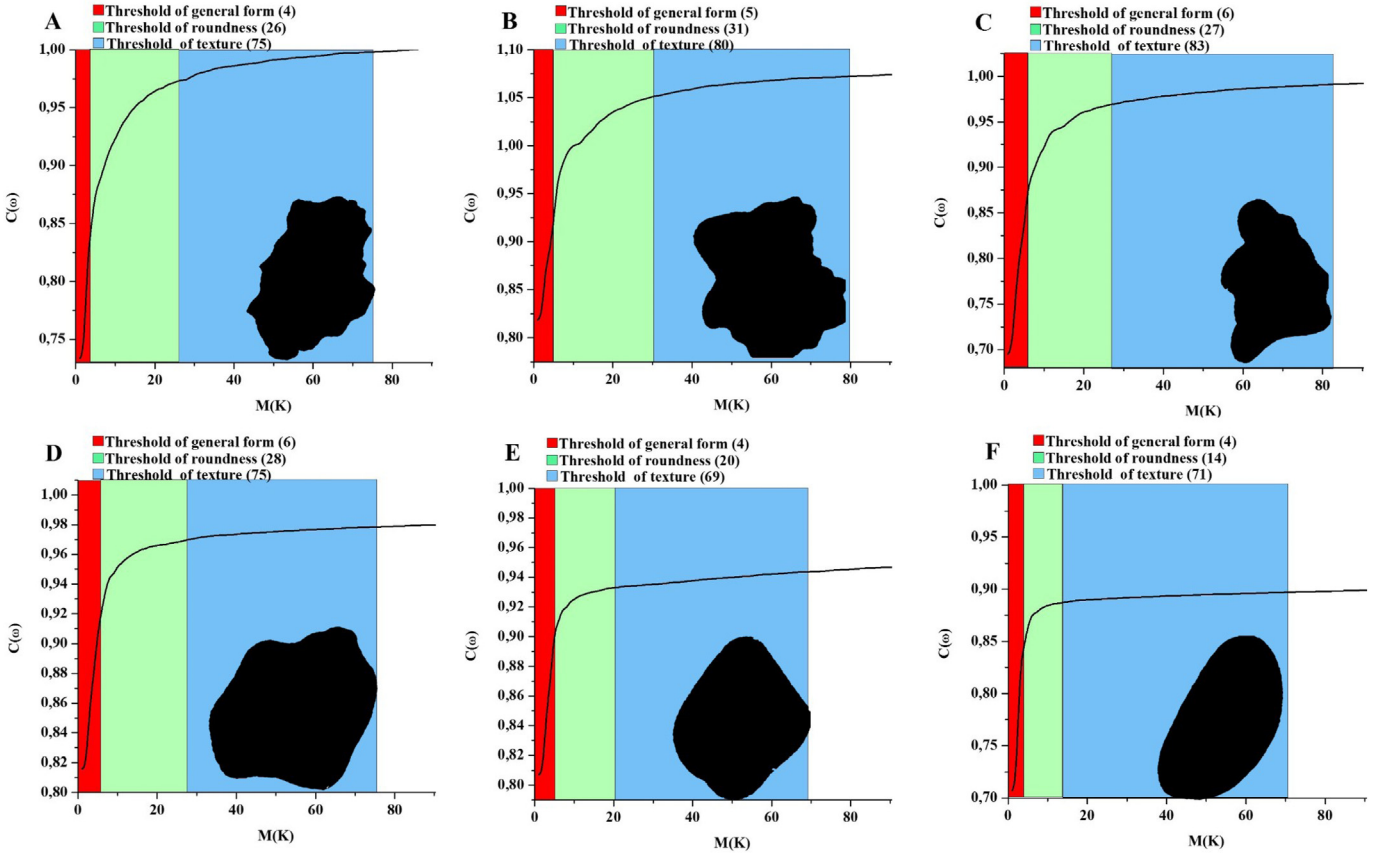

Fig. 7. Analysis of "form," "roundness" and "roughness" applied to six particles. Morphology order ranges are harmonics 4–6 for "form," harmonics 15–31 for "roundness" and harmonics 67–86 for "roughness" (surface texture).

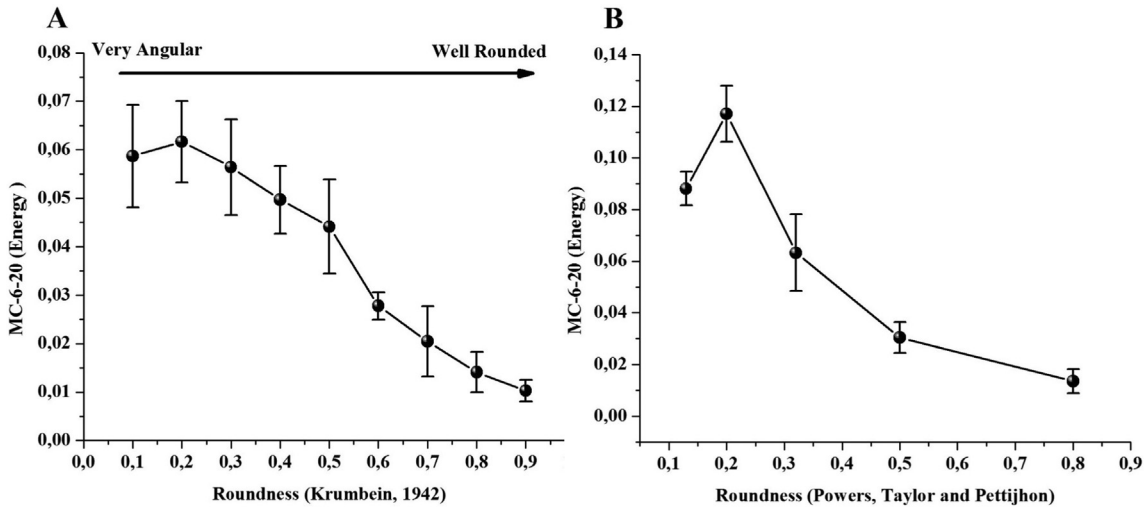

Fig. 8. Graphs showing how the morphological coefficient of harmonics 6–20 is able to distinguish between different "roundness categories" proposed by Krumbein (A) and Powers, Taylor and Pettijohn (B). Fig. B shows that the very angular and angular classes are inverted due to an error in the original reference figures.

on various roundness values of both Krumbein (Fig. 8A) and Powers (Fig. 8B), demonstrating the efficiency of the FSA algorithm for quantitatively measuring the roundness of clastic particles. In Fig. 8B, the FSA algorithm is able to detect an error in the set of reference particles proposed by Powers, Taylor and Pettijohn. This error had been previously detected both using fractals and using Fourier shape analysis (Sarocchi, 2006). It is important to consider that when these images were proposed, the use of quantitative texture analysis techniques was still very limited and unknown to most geologists.

4.2. Discriminating primary and reworked pyroclastic deposits using FSA parameters

The FSA morphological coefficients (described in Appendix A) enable sedimentary and volcano-sedimentary materials to be characterized, outcrops to be correlated or distinguished, and inferences made about transport and fragmentation processes occurring before and during deposit formation. Quantitative textural analysis promises to be an efficient method for discriminating between primary and reworked volcanic mass flow deposits, an important issue for volcano-sedimentology researchers.

In a study of the July 17, 1999 block-and-ash flows (BAF) in the Colima volcano (Sarocchi et al., 2011), distal outcrops showed textural characteristics (including intercalations of finer levels with structures, better sorted parts of the deposits, stains indicating water percolation) that suggested the presence of rework due to water. It is not uncommon for reworked deposits, remobilized and transported by water a few hundred meters, to look like primary deposits.

The morphological coefficients provided by the FSA software were used to measure the morphological characteristics (form, roundness and roughness) of the clasts in these outcrops of uncertain origin. These deposits were compared with other deposits whose origin is well known (from eyewitnesses and studies carried out immediately after the eruption); namely, primary deposits (BAF) and lahars, which are surely reworked (LHR). In order to make this study consistent with the work of Sarocchi et al. (2011), the morphological coefficients MC_{3-6}, MC_{7-15} and MC_{16-50}, which correspond approximately to form, roundness and roughness, were used (Sarocchi, 2007; Sarocchi, 2007). Since clast shape in volcaniclastic deposits changes with grain size (Sarocchi et al., 2011; Caballero et al., 2012), coarser clasts being more rounded, we focused on studying and comparing only the −3 phi class (8–16 mm) of the samples in order to have reproducible data. Using other grain sizes for the study, similar results are obtained, but shifted towards more rounded (coarser clasts) or more angular (finer clasts) morphologies. The important aspect is to compare results obtained within the same grain size ranges.

In the scatter plot in Fig. 9a, morphological coefficients are plotted with "form" (MC_{3-6}) on the abscissa, and "roundness" (MC_{7-15}) on the

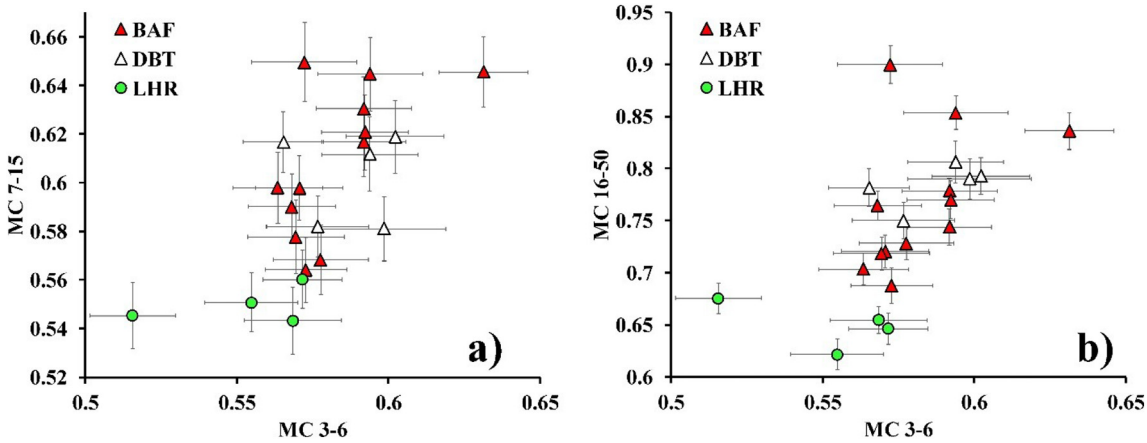

Fig. 9. Discrimination diagrams based on the contraposition of morphological parameters MC_{3-6} (form), parameters MC_{7-15} (roundness) and MC_{16-50} (roughness). It can be seen that the lahar deposit clasts (LHR) that suffered rework are separated from the others. Doubtful clasts (DBT), which were thought to have suffered rework, fall into the field of primary block-and-ash flow clasts (BAF), suggesting that they were probably not reworked by water.

ordinate. In the graph of Fig. 9b, "form" is compared with a morphological coefficient related to roughness (MC_{16-50}). Both graphs show separate regions corresponding to lahars and to primary BAF deposits. All doubtful samples (DBT) fall within primary flow deposit regions, so it is likely that they did not suffer rework. This example shows the potential of this tool in distinguishing primary deposits from reworked deposits based on particle morphology.

5. Discussion about the use of FSA in volcanology

Although the usefulness of FSA methods for detecting even slight morphology variations in clasts has been demonstrated, they have not often been applied to volcanology. The reason probably lies in the lack of available user-friendly software. To date, researchers who used FSA in volcanology have had to develop their own software (Sarocchi, 2007; Sarocchi et al., 2011; Caballero et al., 2012; Charpentier et al., 2013). All existing FSA software produces a power spectrum as output; however, the use to which the harmonic information provided from the spectrum has been put is very diverse. Over time, various types of morphological coefficients have been tested and used. Some authors have linearized the spectrum with respect to a reference spectrum (i.e., calculated for many clasts of different natures) to give the same weight to the different harmonics (Sarocchi et al., 2011; Caballero et al., 2014); other authors have used the spectrum without linearization (Charpentier et al., 2013). The same applies to the harmonics used to describe a specific type of irregularity; some authors have used single harmonics (Sarocchi, 2007; Caballero et al., 2012), others harmonic packages (Sarocchi et al., 2011; Caballero et al., 2012) and others all the harmonics constituting the spectrum (Charpentier et al., 2013). In all cases these coefficients were chosen empirically and not in a standardized way. This being so, the FSA software represents a notable step forward. In addition to allowing the use of custom harmonic packages, it allows packages to be used with thresholds calculated on the basis of a rigorous statistical study of a large set of pyroclastic and epiclastic particles. It also provides adaptive morphological coefficients, where thresholds corresponding to different shape orders are tailored in real time by the software for any specific clast. This contribution to FSA methodology is of paramount importance and concludes a series of empirical experiments on the use of harmonics as morphological coefficients. In addition, FSA software includes in its code a mathematical procedure (Ehrlich and Weinberg, 1970) that limits the classic problem of the bijectivity during sampling of the perimeter. With this measure, the presence of notches in the perimeter does not produce reading errors, unlike previous software.

Some authors (Sarocchi, 2006; Sarocchi et al., 2011; Charpentier et al., 2013), and this work as well, have tested their morphological coefficients with standard clast-shape reference figures (Krumbein, 1941a, 1941b; Powers, 1953). These silhouettes have been commonly used in field geology for semi-quantitative particle morphology study (see Appendix B). Regardless of which Fourier coefficient has been used, the objective of separate figures with different roundness has always been achieved. This result confirms the efficacy of FSA in separating the known shape classes. As proof of its measurement accuracy, we were able to detect an error in Powers's (1953) original figures, where the angular and very-angular classes are inverted. The error was also observed by Sarocchi (2006) using FSA and fractal analysis on these same figures. These studies also point out that more irregular classes in the charts have larger intrinsic error and vice versa.

FSA has great potential in volcanology. The possibility of quantitatively and accurately measuring different morphological characteristics of the clasts may provide longitudinal and vertical variations in the sampling position along a deposit. This enables inferences to be made about rheological conditions in pyroclastic density currents and debris flows during the transport and deposition processes.

Most of the studies carried out to date in volcanology have been oriented only towards measuring changes in particle morphology and relating them to inter-particle interactions and flow conditions. Sarocchi (2007) and Sarocchi et al. (2011), using FSA, focused on BAF clast morphology variations along the San Antonio ravine on the southeast flank of the Colima volcano. They observed that primary PDC material shows a general increase in angularity towards the distal areas of the deposit; however, the same material reworked and transported by a lahar shows progressive rounding. The authors relate these variations to different types of regimes acting in the flow (Sarocchi et al., 2011). These regimes depend on morphometric characteristics of the slopes and ravines, kinematic flow conditions, and flow rheology during transport and deposition. These studies also support the model of a stratified density current where the development of certain morphologies depends on the different types of clast–clast interactions and regimes operating in the flow. A similar mechanism has been documented with FSA methods in lahar deposits. Charpentier et al. (2013) applied these techniques to the La Lumbre ravine on the southwestern slope of the same volcano, showing the relationships between clast morphology and changes in the slope, width and curves of the ravine. Caballero et al. (2012) made a different use of FSA methodology. They performed original experiments on fragmentation, comminution and particle smoothing in a standard rotating drum (Los Angeles machine), studying the evolution in shape, roundness and roughness occurring in different grain size classes along transport (reworking). In their experiments, the authors used mixtures of andesitic material, mixed with different clay (kaolin) content and variable water content. The mixtures showed a range of rheological behavior, from less to more cohesive. Their experiments demonstrated that during the rework process, coarser particles become more equant and more rounded than fine particles. This is evident in many real pyroclastic density currents and lahar deposits. Moreover, this abrasion process appears to be more effective in cohesive flows.

Because of the lack of literature on these methods in volcanology, there are broad areas open for further research. For example, the previous section shows how the FSA morphological coefficients can be a practical way to distinguish primary and reworked deposits, a very common problem for researchers studying PDC deposits. A field that still has to be well explored, and that is very promising, is the classification of volcanic activity involved in pyroclastic deposit formation. It has been seen that the shape of pyroclastic particles (considering particles of the same lithology and size) depends considerably on the type of fragmentation and the style of volcanic activity. A clast morphology study performed on several deposits whose origin is known could help to construct very effective classification diagrams.

We are confident that the software developed here, which is user-friendly, free and open source, as well as the proposed advanced methodology, can encourage many pyroclastic deposit researchers to use and disseminate this powerful tool in volcanology.

6. Conclusions

The FSA software provides a user-friendly tool for rigorous, quantitative textural analysis. It is the first freeware of this type available to the scientific community.

The algorithm used in the code in most cases solves the classic FSA problem of multiple intersections (bijectivity) between the perimeter and the radius used for its sampling. The software is suitable for analyzing complex perimeters with narrow edges and notches, such as pumice or scoria clasts.

The most important contribution of this work is to have found, through a study on more than 3600 natural volcanic particles related to different volcano-sedimentary processes, the harmonic thresholds between different morphological orders (form, roundness, roughness) as proposed by Barrett (1980). These limits have been sought since FSA was first proposed.

All the calculated thresholds fall in the same range of variability (Table 1). The coarser irregularities, corresponding to "form," are

located in the harmonic range 2–5, "roundness" is described in the harmonic range 6–20, and "roughness" is described in the range from harmonic 21 up to where noise begins. The threshold variability for the 3664 analyzed particles is on the order of ±0.89 harmonics for "form", ±6 for "roundness" and ±33 for "roughness".

The limit between roughness and noise has been calculated through the same optimization process and is located at harmonic 82 but with a wide range of variability (±33). Parallel to this value, by means of a specifically designed experiment, another value has been calculated which, for images of good quality (clast perimeters with more than 1000 pixels), places this limit at the 256th harmonic, which is probably closer to reality.

The optimization process that has led to calculation of the boundaries between shape classes is in itself an important, original contribution of this work, as is the code used to superimpose variable irregularity on a simple clast (circle), which can be useful for many studies on particle morphology. Both software and codes are freeware and available here.

The FSA software, freely distributed and available to any sedimentary petrology laboratory, can be very useful for carrying out quantitative texture studies, which in the near future will become increasingly important for characterizing and discriminating volcano-sedimentary and sedimentary deposits in general. Moreover, FSA can be useful in several other fields of science and engineering (astronomy, biology, food engineering, pharmaceutical industry) where quantitative particle shape analysis is needed.

CRediT authorship contribution statement

G. Moreno Chávez: Investigation, Software. **F. Castillo-Rivera:** Formal analysis, Visualization, Writing - review & editing. **J.A. Montenegro-Ríos:** Investigation, Writing - review & editing. **L. Borselli:** Formal analysis, Investigation. **L.A. Rodríguez-Sedano:** Formal analysis, Writing - review & editing, Visualization, Investigation. **D. Sarocchi:** Project administration, Funding acquisition, Writing - review & editing, Investigation.

Declaration of competing interest

The authors declare that they have no known competing financial interests or personal relationships that could have appeared to influence the work reported in this paper.

Acknowledgments

This work has been partially funded by The Royal Society, Newton Advanced Fellowship, Grant NAF\R2\180833 and CONACyT Ciencia Básica CB 2016-286764-T. The author also extends thanks for Retention Grant No. 2019-000010-01NACV-00020. Special thanks to Sylvain Charbonnier and to the anonymous reviewer for the insightful comments that greatly helped to improve this work. We also thank Miss. Margaret H. Schroeder Urrutia for her review of the manuscript.

Appendix A. FSA software description

Fourier Shape Analysis (FSA) is a stand-alone Windows program developed on the MATLAB graphical user interface (GUI). The software is open source and the executable version is freely distributed. It can be downloaded and modified from the public repository at https://github.com/Gamalielmch/FSA. A complete software video-manual is available in the same repository.

A.1. FSA software design

The FSA software flow diagram is presented in Fig. A.1. To perform the analysis using the FSA software, a previously segmented image is required. Then a mapping of the perimeter is made using the method described in Section 2.1. The perimeter is expressed as a magnitude-and-phase signal. Using the FFT, the power spectrum is obtained. The power spectrum information is used in two different ways in the FSA software. 1) LA method (linearization and average), linearizing the power spectrum with respect to the average power spectrum of 3600 volcaniclastic particles, according to the method proposed by Sarocchi et al. (2011). In this case the linearized amplitude values are averaged in the considered range; 2) EN method (energy), where the power spectrum is used without linearization, and the harmonic amplitudes are summed (value defined as energy) in the range under consideration.

A morphological analysis can be carried out using the FSA software using four different sets of harmonics, which can be chosen by the user. The first three sets (a, b and c) use the LA method, and the last (d) uses the EN method. For Method a), users can specify their own set of harmonics. The morphological coefficient (MC) is labeled according to the range of harmonics where it is calculated; e.g., MC_{3-6} is the morphological coefficient obtained by averaging the linearized amplitudes of the harmonics from 3 to 6. Method b) uses three sets of harmonics [3–6, 7–15, 16–50] corresponding to form, roundness and roughness. The harmonic ranges are obtained statistically by the optimization analysis described in Section 2. These values are based on an analysis of more than 3600 volcaniclastic particles. Method c) uses three sets of harmonics [2, 3–8, 30–34], empirically related to elongation, form/roundness and roughness, as used in the previous works of Sarocchi et al. (2011), which provided effective results. Method d) uses adaptive morphological coefficients (AMC), where the limits between one morphological class and the next are not fixed but calculated in real time by an optimization process. This method calculates the cumulative amplitude spectrum (CAS), followed by a noise filter as described in Section 3.2 to separate surface texture and digital noise. An optimization function is used to separate general form from roundness and roundness from roughness. The procedure uses the L-method described in the main text.

The results are presented graphically and numerically, including statistical analysis for an easy interpretation of the results.

The design of the FSA software makes the code reusable and easy to develop and modify. Visual elements such as buttons, text, and axes are declared in the FSA_OpeningFcn function. The visual elements are assigned to a handle so that they can be easy to manipulate, add or remove.

The interface has six menu tabs: Open, Setup, Fourier, Graph, Export and Help. Each menu tab has options that call functions found in the FSA.m. The relationship between menu options and functions is very intuitive. It is easy to remove or add a menu option together with its function in the code. The functions contained in the menu options can call other functions external to the FSA.m. For example, the load_images function calls the external function binarize_image.m based on the Otsu segmentation algorithm. RTmethod.m, insertInImage.m and Lmethod.m are external functions. The purpose of having external functions is so that they can be modified without reprogramming the graphical interface.

A.2. Menu tabs

As mentioned above, the interface has six menu tabs. Each menu tab has functions which we will denote as "function/menu tab."

A.3. Summary description of each important software function

The function "load Images/Open" loads single or multiple images in jpg, tiff, bmp or png format. If the loaded images are not binary, the Otsu segmentation method can be applied in order to segment them. The "complement color/setup" function produces the binary image complement. In order for the image to be analyzed correctly, the background must be 0 (black) and the foreground 1 (white). The "Untouched

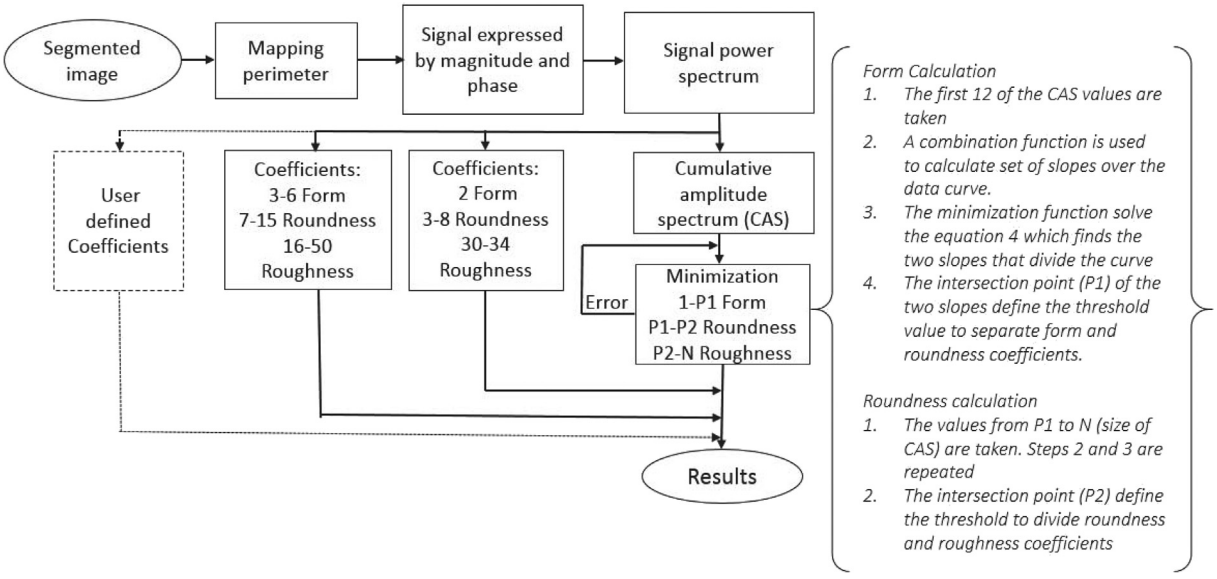

Fig. A.1. Flow diagram of the FSA software algorithm.

edges/setup" function removes objects that touch the image's edges. The "ROI/setup" function enables a region of interest in the image to be selected. The "optimization/Fourier" function applies the functions and methods proposed in the paper. The "mean of image/graph plots" function provides the mean of the sum of spectra of the particles in each image. The "spectrums/export" function saves a spreadsheet with all the particle spectrum data of all the images. The "range stats/export" function saves a spreadsheet with the mean, median, variance and sum of the general form, roundness and roughness ranges. The "labels images/export" function saves an image with the particles labeled and listed. The "documentation/help" function opens the user guide. The user guide, also available separately and downloadable from our webpage (http://www.laima-uaslp.org/), contains detailed information about the FSA software use and its functions.

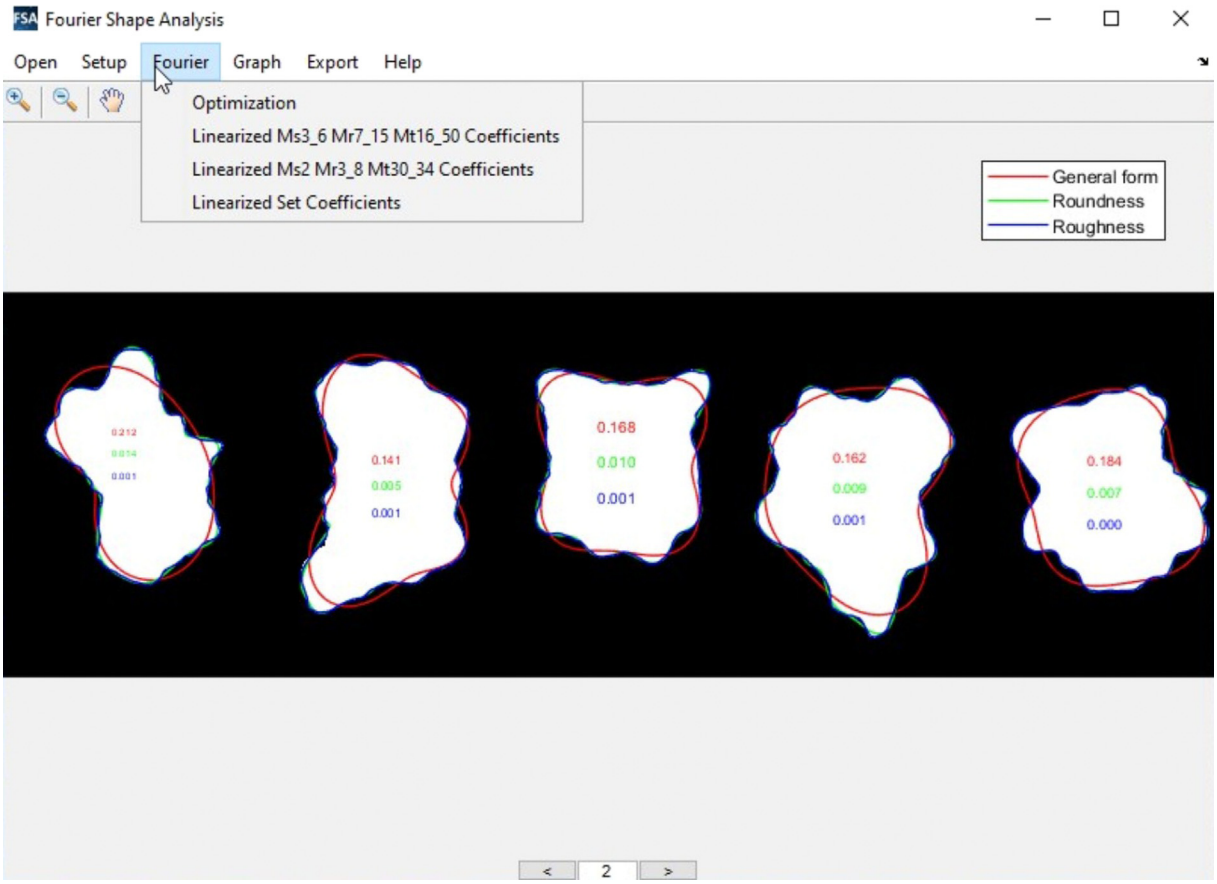

Fig. A.2. Example of the graphical user interface of the FSA software. The menu tabs are at the top and the navigation tools are at the bottom. In the middle are the analyzed clasts with the perimeters corresponding to "general form," "roundness" and "roughness" superimposed with the respective morphological coefficients values displayed for each particle. The Fourier button displays the analysis options, according to different values of thresholds for the harmonics, predefined or definable by the operator.

Appendix B. Standard silhouette charts

In this work, the figures of Krumbein (1941a, 1941b) and Powers (1953) have been used to validate the accuracy of the morphological coefficients provided by the FSA software. These standard silhouettes were drawn in the first half of the last century, in order to make visual comparisons and expeditious semi-quantitative analysis. Their roundness value was calculated by means the Waddell roundness formula:

$$\text{Roundness} = \Sigma(r/R)/N$$

where r is the radius of curvature of grain corners, R is the radius of the largest inscribed circle, and N is the number of corners.

These comparison charts have been widely used in the past and can be considered a reference standard (Lewis and McConchie, 1994; Tucker, 2009). They have been used in volcanology to verify the efficacy of morphological analysis methods (Sarocchi, 2006; Sarocchi et al., 2011; Charpentier et al., 2013). The Krumbein figures (Fig. B.1) are organized into 9 roundness classes (very angular = 0.1 to well-rounded = 0.9) made up of 9 particle silhouettes. Powers's (1953) figures (Fig. B.2), are organized into five roundness classes (angular = 0.1, sub-angular = 0.2, sub-rounded = 0.3, rounded = 0.3 and well-rounded = 0.8), each with five silhouettes with increasing sphericity from left to right.

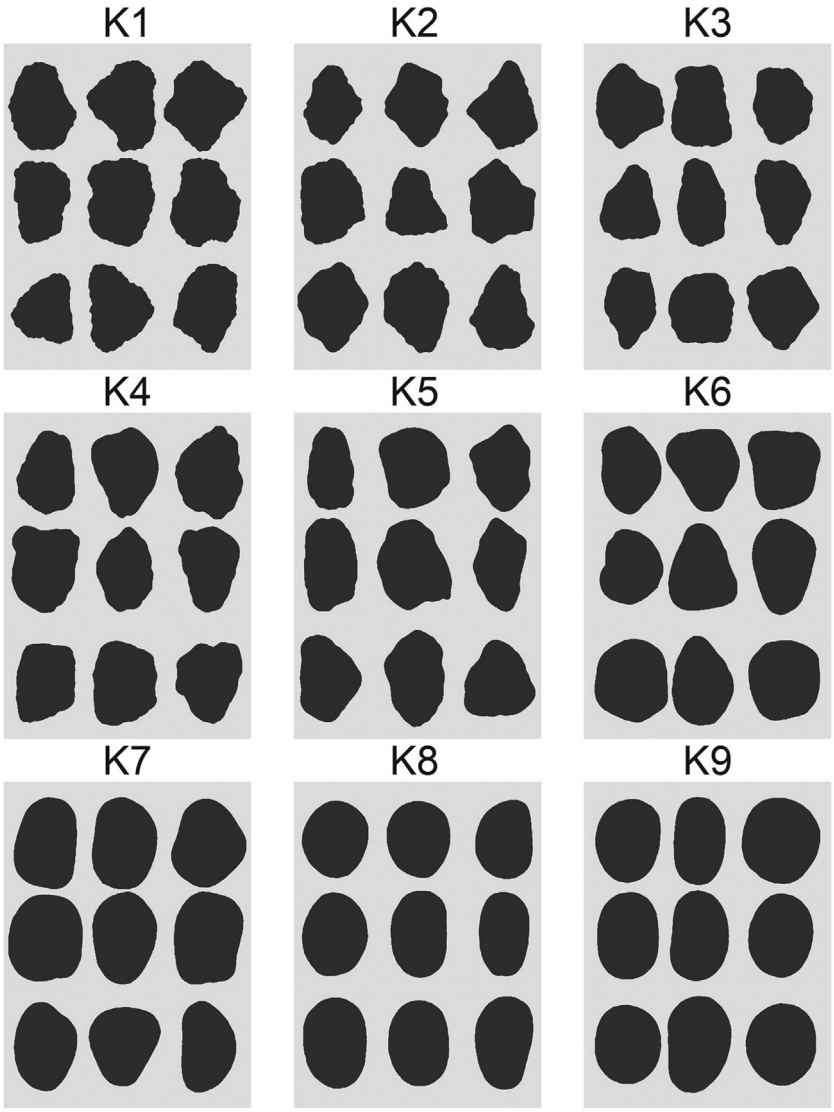

Fig. B.1. Visual comparison silhouettes used to semi-quantitatively assess the degree of roundness, Krumbein (1941a, 1941b). (Drawing modified from Krumbein (1941a, 1941b).)

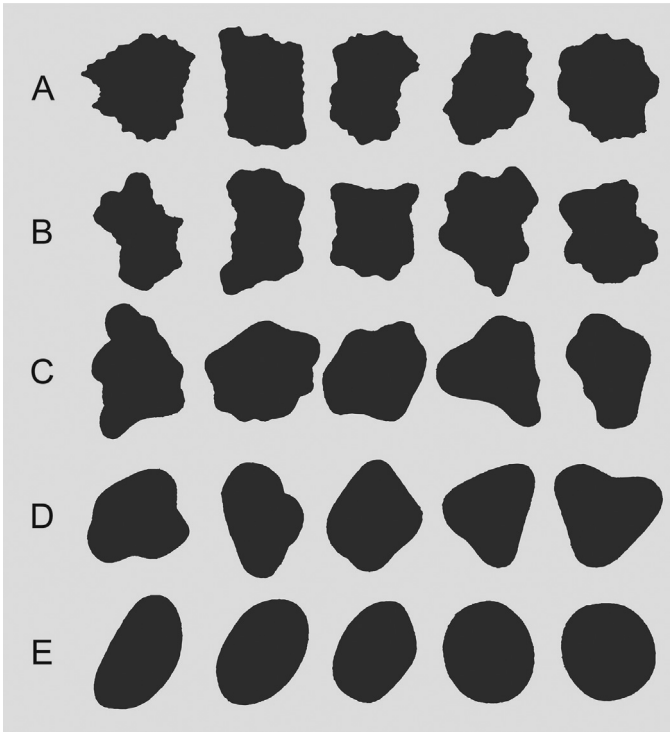

Fig. B.2. Visual comparison silhouettes for roundness and sphericity semi-quantitative estimation proposed by Powers (1953). (A, very angular; B, angular; C, sub-rounded; D, rounded; E, well-rounded.)
(Drawing modified from Powers (1953).)

References

Alshibli, K.A., Alsaleh, M.I., 2004. Characterizing surface roughness and shape of sands using digital microscopy. J. Comput. Civ. Eng. 18, 36–45. https://doi.org/10.1061/(asce)0887-3801(2004)18:1(36).

Bagheri, G.H., Bonadonna, C., Manzella, I., Vonlanthen, P., 2015. On the characterization of size and shape of irregular particles. Powder Technol. 270, 141–153. https://doi.org/10.1016/j.powtec.2014.10.015.

Barclay, D.R., Buckingham, M.J., 2009. On the shapes of natural sand grains. J. Geophys. Res. Solid Earth 114, 1–12. https://doi.org/10.1029/2008JB005993.

Barrett, P.J., 1980. The shape of rock particles, a critical review. Sedimentology 27, 291–303. https://doi.org/10.1111/j.1365-3091.1980.tb01179.x.

Bayhurst, G.K., Wohletz, K.H., Mason, A.S., 1994. A method for characterizing volcanic ash from the December 15, 1989, eruption of Redoubt volcano, Alaska. In: Casadevall, T. (Ed.), Volcanic Ash and Aviation Safety. U.S. Geol. Surv. Bull. vol. 2047, pp. 13–18.

Borselli, 1999. Technical communication segmentation of soil roughness profiles. Earth Surf. Process. Landf. 24, 71–90. https://doi.org/10.7330/9780874219746.c033.

Bracewell, R.N., 1986. The Fourier Transform and Its Applications. vol. 31999. McGraw-Hill, New York.

Caballero, L., Sarocchi, D., Borselli, L., Cárdenas, A.I., 2012. Particle interaction inside debris flows: evidence through experimental data and quantitative clast shape analysis. J. Volcanol. Geotherm. Res. 231–232, 12–23. https://doi.org/10.1016/j.jvolgeores.2012.04.007.

Caballero, L., Sarocchi, D., Soto, E., Borselli, L., 2014. Rheological changes induced by clast fragmentation in debris flows. J. Geophys. Res. Earth Surf. 119 (9), 1800–1817. https://doi.org/10.1002/2013JF002942 (ISO 690).

Capaccioni, B., Sarocchi, D., 1996. Computer-assisted image analysis on clast shape fabric from the Orvieto-Bagnoregio ignimbrite (Vulsini District, central Italy): implications on the emplacement mechanisms. J. Volcanol. Geotherm. Res. 70, 75–90. https://doi.org/10.1016/0377-0273(95)00049-6.

Charpentier, I., Sarocchi, D., Rodriguez Sedano, L.A., 2013. Particle shape analysis of volcanic clast samples with the Matlab tool MORPHEO. Comput. Geosci. 51, 172–181. https://doi.org/10.1016/j.cageo.2012.07.015.

Cioni, R., Pistolesi, M., Bertagnini, A., Bonadonna, C., Hoskuldsson, A., Scateni, B., 2014. Insights into the dynamics and evolution of the 2010 Eyjafjallajökull summit eruption (Iceland) provided by volcanic ash textures. Earth Planet. Sci. Lett. 394, 111–123. https://doi.org/10.1016/j.epsl.2014.02.051.

Davis, J.C., 1986. Statistics and Data Analysis in Geology. John Wiley & Sons, New York.

Dellino, P., La Volpe, L., 1996. Image processing analysis in reconstructing fragmentation and transportation mechanisms of pyroclastic deposits. The case of Monte Pilato-Rocche Rosse eruptions, Lipari (Aeolian islands, Italy). J. Volcanol. Geotherm. Res. 71, 13–29. https://doi.org/10.1016/0377-0273(95)00062-3.

Dellino, P., Liotino, G., 2002. The fractal and multifractal dimension of volcanic ash particles contour: a test study on the utility and volcanological relevance. J. Volcanol. Geotherm. Res. 113 (1–2), 1–18. https://doi.org/10.1016/S0377-0273(01)00247-5.

Dellino, P., Gudmundsson, M.T., Larsen, G., Mele, D., Stevenson, J.A., Thordarson, T., Zimanowski, B., 2012. Ash from the Eyjafjallajökull eruption (Iceland): fragmentation processes and aerodynamic behavior. J. Geophys. Res. Solid Earth 117 (B9). https://doi.org/10.1029/2011JB008726.

Diepenbroek, M., Bartholomä, A., Ibbeken, H., 1992. How round is round? A new approach to the topic 'roundness' by Fourier grain shape analysis. Sedimentology 39, 411–422. https://doi.org/10.1111/j.1365-3091.1992.tb02125.x.

Ehrlich, R., Weinberg, B., 1970. An exact method for characterization of grain shape. J. Sediment. Petrol. 40, 205–212. https://doi.org/10.1306/74D71F1E-2B21-11D7-8648000102C1865D (ISO 690).

Erdoğan, S.T., Garboczi, E.J., Fowler, D.W., 2007. Shape and size of microfine aggregates: X-ray microcomputed tomography vs. laser diffraction. Powder Technol. 177 (2), 53–63. https://doi.org/10.1016/j.powtec.2007.02.016.

Ersoy, O., 2010. Surface area and volume measurements of volcanic ash particles by SEM stereoscopic imaging. J. Volcanol. Geotherm. Res. 190 (3–4), 290–296. https://doi.org/10.1016/j.jvolgeores.2009.12.006.

Full, W.E., Ehrlich, R., Kennedy, S.K., 1984. Optimal configuration and information content of sets of frequency distribution. J. Sediment. Petrol. 54 (1), 117–126. https://doi.org/10.1306/212F83BE-2B24-11D7-8648000102C1865D.

Haines, J., Mazzullo, J., 1988. The original shapes of quartz silt grains: a test of the validity of the use of quartz grain shape analysis to determine the sources of terrigenous silt in marine sedimentary deposits. Mar. Geol. 78, 227–240. https://doi.org/10.1016/0025-3227(88)90111-9.

Heiken, G., Wohletz, K., 1985. Volcanic Ash. University Presses of California, Chicago, Harvard & MIT.

Kaye, 1999. Characterization of Powders and Aerosols. Wiley-VCH GmbH, Weinheim, Germany https://doi.org/10.1002/9783527614028 323 pp.

Krumbein, W.C., 1941a. Measurement and geological significance of shape and roundness of sedimentary particles. SEPM J. Sediment. Res. Vol. 11, 64–72. https://doi.org/10.1306/d42690f3-2b26-11d7-8648000102c1865d.

Krumbein, W.C., 1941b. The Effects of Abrasion on the Size, Shape and Roundness of Rock Fragments. The University of Chicago Press http://www.jstor.org/stable/30069332.

Lees, G., 1964. A new method for determining the angularity of particles. Sedimentology 3, 2–21. https://doi.org/10.1111/j.1365-3091.1964.tb00271.x.

Leibrandt, S., LePennec, J.L., 2015. Towards fast and routine analyses of volcanic ash morphometry for eruption surveillance applications. J. Volcanol. Geotherm. Res. 297, 11–27. https://doi.org/10.1016/j.jvolgeores.2015.03.014.

Lewis, D.W., McConchie, D., 1994. Analytical Sedimentology. Chapman & Hall, New York, pp. 1–197.

Lukas, S., 2013. Clast shape analysis and clast transport paths in glacial environments: a critical review of methods and the role of lithology. Earth Sci. Rev. 121, 96–116. https://doi.org/10.1016/j.earscirev.2013.02.005.

Manga, M., Patel, A., Dufek, J., 2011. Rounding of pumice clasts during transport: field measurements and laboratory studies. Bull. Volcanol. 73, 321–333. https://doi.org/10.1007/s00445-010-0411-6.

Maria, A., Carey, S., 2002. Using fractal analysis to quantitatively characterize the shapes of volcanic particles. J. Geophys. Res. Solid Earth 107 (B11), ECV-7. https://doi.org/10.1029/2001JB000822.

Maria, A., Carey, S., 2007. Quantitative discrimination of magma fragmentation and pyroclastic transport processes using the fractal spectrum technique. J. Volcanol. Geotherm. Res. 161 (3), 234–246. https://doi.org/10.1016/j.jvolgeores.2006.12.006.

Mazzullo, J.J.M., Sims, D., Cunningham, D., 1986. The effects of eolian sorting and abrasion upon the shapes of fine quartz sand grains. J. Sediment. Res. 56 (1), 45–56. https://doi.org/10.1306/212F887D-2B24-11D7-8648000102C1865D.

Montenegro Ríos, A., Sarocchi, D., Nahmad-Molinari, Y., Borselli, L., 2013. Form From Projected Shadow (FFPS): an algorithm for 3D shape analysis of sedimentary particles. Comput. Geosci. 60, 98–108. https://doi.org/10.1016/j.cageo.2013.07.008.

Muller, 1967. In: Stuttgart Muller, G. (Ed.), Methods in Sedimentary Petrology Hafner Publishing Company. vol. 1967, p. 1967.

Nyquist, H., 2002. Certain topics in telegraph transmission theory. Trans. Am. Inst. Electr. Eng. 90, 280–305. https://doi.org/10.1109/T-AIEE.1928.5055024.

Otsu, 1979. A threshold selection method from gray-level histograms. IEEE Trans. Syst. Man, and, Cybern. SMC-9, pp. 62–66 https://doi.org/10.1109/TSMC.1979.4310076.

Powers, M.C., 1953. A new roundness scale for sedimentary particles. SEPM J. Sediment. Res. 23, 117–119. https://doi.org/10.1306/d4269567-2b26-11d7-8648000102c1865d.

Proakis, J.G., Manolakis, D.G., 2004. Digital Signal Processing. 4th edition. PHI publication.

Russ, J.C., 1990. Computer-assisted Microscopy: The Measurement and Analysis of Images. Plenum Press, New York https://doi.org/10.1007/978-1-4613-0563-7.

Salvador, S., Chan, P., 2004. Determining the number of clusters/segments in hierarchical clustering/segmentation algorithms. 16th IEEE International Conference on Tools With Artificial Intelligence, Boca Raton, FL, USA, pp. 576–584 https://doi.org/10.1109/ICTAI.2004.50.

Sarocchi, D., 2006. Análisis textural del depósito de flujo de bloques y cenizas del 17 de julio de 1999 en el Volcán de Colima. PhD Thesis. Posgrado en Ciencias de la Tierra, Inst. Geofísica Universidad Nacional Autónoma de México, p. 143.

Sarocchi, D., 2007. Estudio sedimentológico del depósito de flujo de bloques y ceniza del 17 de julio de 1999 en el volván de Colima. Monografía del Instituto de Geofísica, Vol. 11- UNAM. IGEF-UNAM Ed, México, p. 92.

Sarocchi, D., Sulpizio, R., Macías, J.L., Saucedo, R., 2011. The 17 July 1999 block-and-ash flow (BAF) at Colima Volcano: new insights on volcanic granular flows from textural analysis. J. Volcanol. Geotherm. Res. 204, 40–56. https://doi.org/10.1016/j.jvolgeores.2011.04.013.

Scasso, R.A., Carey, S., 2005. Morphology and Formation of Glassy Volcanic Ash From the August 12–15, 1991 Eruption of Hudson Volcano, Chile.

Schwarcz, H.P., Shane, K.C., 1969. Measurement of particle shape by Fourier analysis. Sedimentology 13, 213–231. https://doi.org/10.1111/j.1365-3091.1969.tb00170.x.

Tucker, M.E. (Ed.), 2009. Sedimentary Petrology: An Introduction to the Origin of Sedimentary Rocks. John Wiley & Sons.

Tunwal, M., Mulchrone, K.F., Meere, P.A., 2020. Image based Particle Shape Analysis Toolbox (IPSAT). Comput. Geosci. 135, 104391. https://doi.org/10.1016/j.cageo.2019.104391.

Wadell, H., 1933. Volume, shape, and roundness of quartz particles. J. Geol. 41, 310–331.

Wentworth, C.K., 1919. A laboratory and field study of cobble abrasion. J. Geol. 27 (7), 507–521. https://www.jstor.org/stable/30058414.

Winkelmolen, A.M., 1982. Critical remarks on grain parameters, with special emphasis on shape. Sedimentology 29, 255–265. https://doi.org/10.1111/j.1365-3091.1982.tb01722.x.

Wohletz, K.H., 1983. Mechanisms of hydrovolcanic pyroclast formation: grain-size, scanning electron microscopy, and experimental studies. J. Volcanol. Geotherm. Res. 17 (1–4), 31–63. https://doi.org/10.1016/0377-0273(83)90061-6.